https://doi.org/10.5194/mr-2024-7
Preprint. Discussion started: 9 April 2024

Open Access MAGNETIC RESONANCE Discussions

Analysis of chi angle distributions in isolated amino acids via multiplet fitting of proton scalar couplings

Nabiha R. Syed[1], Nafisa B. Masud[1], and Colin A. Smith[1]

[1]Department of Chemistry, Wesleyan University, Middletown, CT, United States

Correspondence: Colin A. Smith (colin.smith@wesleyan.edu)

Abstract. Scalar couplings are a fundamental aspect of nuclear magnetic resonance (NMR) experiments and provide rich information about electron-mediated interactions between nuclei. ^3J couplings are particularly useful for determining molecular structure through the Karplus relationship, a mathematical formula used for calculating ^3J coupling constants from dihedral angles. In small molecules, scalar couplings are often determined through analysis of one-dimensional proton spectra. Larger proteins have typically required specialized multidimensional pulse programs designed to overcome spectral crowding and multiplet complexity. Here we present a generalized framework for fitting scalar couplings with arbitrarily complex multiplet patterns using a weak coupling model. The method is implemented in FitNMR and applicable to 1D, 2D, and 3D NMR spectra. To gain insight into the proton-proton coupling patterns present in protein side chains, we analyze a set of isolated amino acid 1D spectra. We show that the weak-coupling assumption is largely sufficient for fitting the majority of resonances, although there are notable exceptions. To enable structural interpretation of all couplings, we extend a self-consistent Karplus parameterization of side chain chi 1 to chi 2-4. An enhanced model of side chain motion incorporating rotamer statistics from the Protein Data Bank (PDB) is developed. Even without stereospecific assignments of the beta hydrogens, we find that two couplings are sufficient to exclude a single-rotamer model for all amino acids except proline. While most isolated amino acids show rotameric populations consistent with crystal structure statistics, beta-branched valine and isoleucine deviate substantially.

1 Introduction

The structure and dynamics of amino acid side chains is often critical for protein function. Side chains are not only an important part of the folded structure of proteins, but also key in facilitating molecular recognition, allosteric regulation, and catalysis. Nuclear magnetic resonance (NMR) is a particularly powerful technique for studying side chains as they move in solution at physiological temperatures. ^3J scalar couplings give the most direct information about the local structure of side chains through the mathematical relationship between the dihedral angles of rotatable bonds and ^3J, which was originally formulated by Karplus (1963). The numerous NMR experiments for measuring protein scalar couplings have been reviewed in detail by Vuister et al. (2002). Notably, it is possible to measure every scalar coupling involved in the side chain chi 1 angle, including ^3J(HA-HB), ^3J(C-HB), ^3J(N-HB),^3J(HA-CG), ^3J(N-CG), and ^3J(C-CG). (Protein Data Bank (PDB) atom names are used throughout this manuscript.)

https://doi.org/10.5194/mr-2024-7
Preprint. Discussion started: 9 April 2024

Open Access MAGNETIC RESONANCE Discussions

Homonuclear proton-proton couplings, which are the focus of the present study, result in sometimes complex multiplet patterns in one-dimensional proton NMR spectra. Numerous pulse sequences have been developed to overcome this complexity and make proton-proton couplings easier to resolve and quantify in multidimensional spectra. The first was Exclusive Correlation Spectroscopy (E.COSY) (Griesinger et al., 1985, 1986, 1987), which generates cross-peak multiplets with reduced numbers of peaks and takes advantage of passive couplings to make line splitting by the active coupling visible for inspection and quantification. For ^{13}C-labeled samples, this idea was extended using modified versions of the HCCH-COSY and HCCH-TOCSY experiments, where ^{1}J(C-H) was used to resolve ^{3}J(H-H). (Gemmecker and Fesik, 1991; Griesinger and Eggenberger, 1992; Emerson and Montelione, 1992) An HXYH experiment further improved experimental efficiency by simultaneously measuring both backbone and side chain ^{3}J couplings using ^{13}C^{15}N-labeled proteins. (Tessari et al., 1995; Löhr et al., 1999) Another class of experiments, quantitative J correlation, use the ratio between a diagonal and cross peak to determine the value of the coupling constant, first demonstrated with the HNHA experiment which measures the backbone ^{3}J(H-HA). (Vuister and Bax, 1993) An HACACB-COSY adaptation of this technique enabled quantification of side chain couplings. (Grzesiek et al., 1995)

Another approach for obtaining scalar couplings uses numerical processing of a pair of matched experimental spectra, one having in-phase peaks with the same sign and the other having anti-phase peaks with opposite signs. (Oschkinat and Freeman, 1984; Kessler et al., 1985; Titman and Keeler, 1990; Huber et al., 1993; Prasch et al., 1998) In these methods, a pair of trial anti-phase/in-phase peaks are convolved with a multiplet in the respective spectra. The coupling is determined by finding the separation between the trial peaks that results in maximum agreement between the two convolved spectra. However, peak overlap can be a problem with these types of methods because only a single multiplet is analyzed at a time.

Various approaches have been applied to directly fit peak multiplets that can handle peak overlap. SpinEvolution (Veshtort and Griffin, 2006), Quantum Mechanical Total-Line-Shape Fitting (QMTLS) in PERCH (PERCH Solutions), ChemAdder (Tiainen et al., 2014), Guided Ideographic Spin System Model Optimization (GISSMO) (Dashti et al., 2017, 2018), ANATOLIA (Cheshkov et al., 2018), and Cosmic Truth (NMR Solutions) (Achanta et al., 2021) enable fitting of a one-dimensional spectrum by iteratively optimizing parameters used to simulate the spectrum using a quantum mechanical description of the spin system(s). (Castellano and Bothner-By, 1964; Heinzer, 1977; Cheshkov and Sinitsyn, 2020) Such calculations account for cases where the chemical shift difference between two nuclei approach the value of their scalar coupling. This leads to strong coupling and the so-called “roofing effect” where peaks in the multiplet closest to the other nucleus increase in intensity and those farthest decrease in intensity. While such calculations are usually computationally intensive, methods have been developed to very rapidly simulate 1D spectra. (Castillo et al., 2011) Global Spectral Deconvolution (GSD) in Mnova NMR (Mestrelab Research) enables fitting individual peaks in 1D spectra and classification of peaks into multiplets. (Bernstein et al., 2013) More recently, deep neural networks have been combined with lineshape fitting to automatically quantify peaks in 1D spectra. (Li et al., 2023)

Several methods exist for fitting multidimensional spectra including PINT (Ahlner et al., 2013; Niklasson et al., 2017) and INFOS (Smith, 2017), but those tools do not explicitly model scalar couplings. Amplitude-Constrained Multiplet Evaluation (ACME) was developed to fit proton-proton scalar couplings in COSY cross peaks. (Delaglio et al., 2001) Explicit modeling

https://doi.org/10.5194/mr-2024-7
Preprint. Discussion started: 9 April 2024

Open Access MAGNETIC RESONANCE Discussions

of scalar couplings in multidimensional spectra can also be done in Spinach (Hogben et al., 2011), which is a widely used software library optimized for simulations of large spin systems. However, like the commercially available NMRSim (Bruker) that can also simulate multidimensional spectra, the calculations can be time-consuming and are not typically used for direct spectral fitting.

Once accurate ^3J couplings have been measured and quantified, they can be interpreted using the Karplus relationship, which relates ^3J to a linear combination of $\cos\theta$ and either $\cos 2\theta$ or $\cos^2\theta$, where θ is the dihedral angle between the coupled nuclei. The three coefficients (a constant and two scaling factors for the cos functions) determine the Karplus parameterization. The coefficients have been most often determined using a large set scalar coupling measurements for which coordinates from X-ray crystallography are also available. A structure-free approach to parameterizing scalar couplings was developed by Schmidt et al. (1999). It depends on the measurement of many different scalar couplings, each with a different relationship to the overall dihedral angle. By having many scalar couplings, both the dihedral angles of the chemical bonds and the associated Karplus parameters can be determined in a self-consistent manner. This approach was originally applied to scalar couplings in the protein backbone (Schmidt et al., 1999) and then expanded to side chains (Pérez et al., 2001).

The ^3J(H-HA) scalar coupling is dependent on the phi backbone dihedral angle and takes distinct values depending on whether the residue is part of an alpha helix or beta sheet. In most heteronuclear NMR spectra, the power output required for decoupling ^{13}C and/or ^{15}N in isotopically labeled proteins limits the direct-dimension acquisition time, leading to signal truncation that hinders resolution of the ^3J(H-HA) line splitting. Increasing molecular size also broadens the linewidths, further exacerbating the resolution. However, we recently showed that through very precise modeling of signal truncation and apodization, ^3J(H-HA) could be quantified in ordinary ^{1}H$-^{15}$N 2D spectra using nonlinear least squares fitting in FitNMR. (Dudley et al., 2020) A byproduct of this fitting is that the ^{1}H transverse relaxation rate, R_2^*, can also be quantified, which can provide valuable information about protein structure and dynamics. (Dudley et al., 2024)

Towards the ultimate goal of being able to similarly quantify side-chain ^{1}H scalar couplings and R_2^* values directly from multidimensional spectra of folded proteins, as well as extract accurate volumes for highly overlapped peaks, we present an analysis of the proton-proton couplings in ^{1}H spectra of individual amino acids. We describe how FitNMR was enhanced to directly model complex multiplet patterns in multidimensional spectra using a simple tabular input/output format. The strengths and weaknesses of using a model that assumes purely weak-coupling interactions are illustrated. To obtain Karplus parameters, we extend a self-consistent parameterization of ^3J(HA-HB) couplings to include ^3J(HB-HG), ^3J(HG-HD), and ^3J(HD-HE). Finally, we apply an enhanced model of side chain motion incorporating prior rotameric information to determine differences in the conformational preferences between the side chains of isolated amino acids and those found in crystal structures.

2 Methods

2.1 Fitting couplings in multidimensional spectra

FitNMR (Dudley et al., 2020) was originally designed such that each peak in a multiplet would be a distinct entity. To allow for scalar couplings, the chemical shifts of a given peak could be made linear combinations of auxiliary chemical shift parameters,

https://doi.org/10.5194/mr-2024-7
Preprint. Discussion started: 9 April 2024

Open Access MAGNETIC RESONANCE Discussions

Table 1. Isoleucine resonances table

	x	x_sc	1_m0
HA	HA	HA-HB	859348095
HB	HB	HA-HB HB-HG12 HB-HG13 HB-HG2 HB-HG2 HB-HG2	978275274
HG12	HG12	HB-HG12 HG12-HG13 HG12-HD1 HG12-HD1 HG12-HD1	1099447740
HG13	HG13	HB-HG13 HG12-HG13 HG13-HD1 HG13-HD1 HG13-HD1	1088697294
HG2	HG2	HB-HG2	3413052104
HD1	HD1	HG12-HD1 HG13-HD1	3213059843

Table 2. Isoleucine nuclei table

	omega0_ppm	r2_hz
HA	3.595	0.565
HB	1.908	0.772
HG12	1.396	0.715
HG13	1.187	0.696
HG2	0.936	0.654
HD1	0.864	0.637

whose coefficients were chosen such that a scalar coupling in Hz could be mapped onto the ppm scale. While this functioned well for fitting simple doublets found in protein $^{1}H-^{15}N$ 2D spectra, it did not scale well to other applications, especially complicated spectra with heterogeneous coupling patterns.

To address this, we developed a new way of defining NMR spectral features, for which we use the term resonances. They are defined in a comma separated values (CSV) `resonances` text file, with an example for isoleucine shown in Table 1. The first column gives the name of the resonance, which can be arbitrarily defined. FitNMR supports up to four spectral dimensions, referred to using the names `x`, `y`, `z`, and `a`, following nomenclature used by NMRPipe (Delaglio et al., 1995). The particular nucleus associated with each dimension is given in the column with the same name as the dimension. Scalar couplings active in each dimension are given in a corresponding column whose name has the `_sc` suffix. They are space delimited and can also be arbitrarily named, although no nucleus and scalar coupling may share the same name. A scalar coupling can appear several times to produce canonical multiplets like triplets, quartets, etc. For instance, in isoleucine the HB resonance definition produces a doublet of doublets of doublets of quartets, with couplings to HA, HG12, HG13 each producing a doublet and couplings to the HG2 methyl group producing a quartet. Additional columns give the volumes associated with individual spectra, referred to by FitNMR as `m0` (initial magnetization).

https://doi.org/10.5194/mr-2024-7
Preprint. Discussion started: 9 April 2024


Open Access MAGNETIC RESONANCE Discussions

Table 3. Isoleucine scalar couplings table

	hz
HA-HB	3.95
HB-HG12	4.83
HB-HG13	9.29
HB-HG2	7.02
HG12-HG13	-13.49
HG12-HD1	7.47
HG13-HD1	7.36

Each nucleus referred to in the `resonances` table is defined in the `nuclei` table, with an example for isoleucine shown in Table 2. The first column gives the nucleus name. The second `omega0_ppm` column gives the chemical shift offset, Ω_0, in ppm. The third `r2_hz` column gives the transverse relaxation rate (including an inhomogeneous contribution), R_2^*, in Hz. The coupling table (Table 3) just has a single `hz` data column with the value of the scalar coupling in Hz.

2.2 Fitting amino acid 1D spectra

Starting parameters for fitting amino acid 1D NMR spectra were adapted from the Guided Ideographic Spin System Model Optimization (GISSMO) database (Dashti et al., 2017, 2018), with couplings added or removed as appropriate. Chemical shifts were manually altered to account for differences in referencing and effects of strong coupling which FitNMR does not currently model. Standard PDB atom names were used. When two nonmethyl protons were modeled with a single chemical shift, their respective numbers were separated by a slash. For methyl protons, the last number identifying each proton was dropped from the name. Geminal proton names were assigned to follow the ordering observed in BMRB statistics (https://bmrb.io/histogram/) and do not reflect a stereospecific analysis of the fitted ^3J coupling values.

Fitting was done with the `refit_peaks.R` script from FitNMR 0.7. The spectra were fit in a region ± 0.02 ppm from the starting peaks in each multiplet. The chemical shift was allowed to move up to 3.5 times the starting R_2^* during fitting. R_2^* was constrained to be 0.1 to 2 Hz and the scalar couplings were constrained to be -20 to 20 Hz.

2.3 Karplus parameters for side chain chi angles

When spanning a rotatable bond, ^3J scalar couplings provide information about the dihedral angle (θ) between the two coupled atoms through the well-known Karplus relationship (Karplus, 1963):

$$^3J(\theta) = C_0 + C_1 \cos\theta + C_2 \cos 2\theta \quad (1)$$

An alternative formulation of the Karplus relationship dependent on $\cos\theta$ and $\cos^2\theta$ terms is often used, but here we apply the originally proposed relationship which is derived from a truncated Fourier series. A parameterization of the coefficients

https://doi.org/10.5194/mr-2024-7
Preprint. Discussion started: 9 April 2024


Open Access MAGNETIC RESONANCE Discussions

for side chain chi 1 angles was previously developed (Pérez et al., 2001) in which the average scalar coupling given by the C_0 coefficient is perturbed by set of increments ($\Delta C_{0,i}$) weighted by the number (N_i) of proton/heavy atom substitutions made around the bond for a particular element type i:

$$^3J(\theta) = C_0 + \sum(N_i \Delta C_{0,i}) + C_1 \cos\theta + C_2 \cos 2\theta \quad (2)$$

This formulation makes it possible to extrapolate the parameterization to chemical substructures outside the training set. For proton-proton ^3J couplings, the following previously determined (Pérez et al., 2001) coefficients and coefficient increments were used: $C_0 = 7.24$, $C_1 = -1.37$, $C_2 = 3.61$, $\Delta C_{0,\mathrm{C}} = 0.61$, $\Delta C_{0,\mathrm{O}} = -1.59$, and $\Delta C_{0,\mathrm{S}} = -1.30$ Hz. The offset for nitrogen atoms was previously defined $\Delta C_{0,\mathrm{N}} = 0$ Hz because $N_\mathrm{N} = 1$ for all side chain chi 1 angles, making it impossible to separate the contribution of a nitrogen substitution from the fundamental Karplus coefficient C_0.

The θ angle refers to the dihedral angle between the two coupled protons, which is often offset from the canonical side chain chi angle (χ) by a given value, $\Delta\chi$:

$$\theta = \chi + \Delta\chi$$

For the chi 1 dihedral angle, the $\Delta\chi$ and heavy atom substitution counts were previously published. (Pérez et al., 2001) For this work, we determined a complete set of parameters necessary for Karplus analysis of proton-proton couplings associated with chi 1-4 by analyzing representative amino acid structures taken from the PDB Chemical Component Directory (CCD). (Westbrook et al., 2015) An example representative structure for isoleucine is shown in Figure 1A and the parameters determined for all amino acids are given in Table A2.

2.4 Chi angle distribution analysis

During self-consistent parameterization of the side chain Karplus parameters (Pérez et al., 2001), two different models of motion were previously used. Model M_1 involved normally distributed fluctuation about a mean $\chi 1$ angle with standard deviation $\sigma_{\chi 1}$. Model M_2 assumed jumps between 60°, 180°, and 300° and varied the respective populations. Each model had two free parameters and M_1 was used for determining the final published parameters.

Here, we also apply a third model (which we call M_3) involving jumps between three rotameric bins whose chi angle distributions were taken from the 2010 Dunbrack rotamer library. (Shapovalov and Dunbrack, 2011) The M_3 model used 610,177 different side chain conformations from their dataset. For each side chain conformation, the theoretical coupling value was calculated using Equation 2 and the data from Table A2. Depending on the application, these theoretical couplings were averaged over all rotamers (as done for Figure 3) or the three different rotameric bins associated with chi 1 (as done for Figure 4).

https://doi.org/10.5194/mr-2024-7
Preprint. Discussion started: 9 April 2024

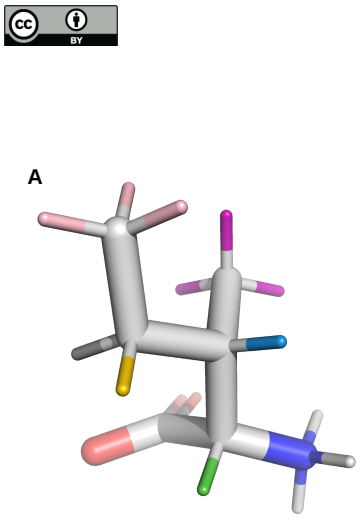

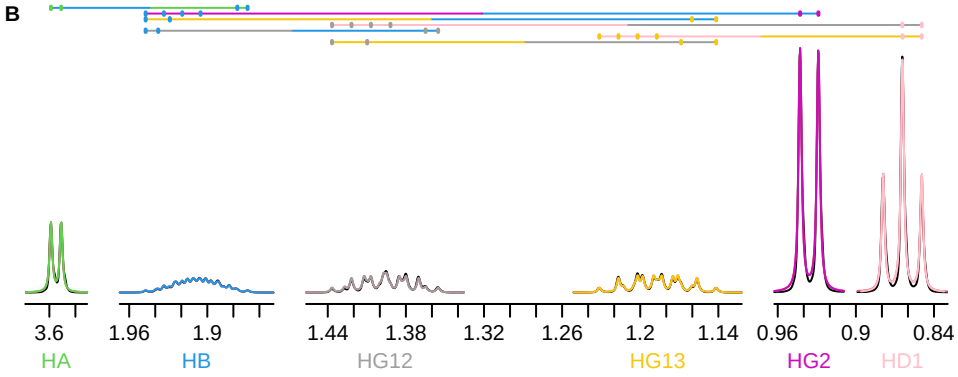

Figure 1. A) Representative structure of isoleucine taken from the CCD with the termini made zwitterionic in PyMOL. Protons are grouped by color, with each color having a distinct chemical shift modeled by a single resonance in the fit. The NH_3^+ hydrogens (white) are deuterated due to exchange with D_2O. **B)** Fit of 500 MHz ^1H NMR spectrum of isoleucine in D_2O as described by Tables 1-3. The experimental spectrum is shown in black and the modeled signal corresponding to each resonance is shown with the same color as in **A**. Each scalar coupling is represented by a horizontal line above the spectrum, with the colors matched to the group being coupled to. The outermost multiplet produced by each coupling is represented by vertical dashes. The x-axis gives the ^1H chemical shift in ppm using a sparse representation. This panel was produced with the `plot_sparse_1d` FitNMR function.

3 Results and Discussion

3.1 Fitting amino acid 1D spectra

To gain insight into coupling patterns between carbon-bound protons in amino acid side chains, we performed fits of spectra taken from the Biological Magnetic Resonance Databank (BMRB) (Hoch et al., 2023). (Table A1) The samples contained individual amino acids dissolved in D_2O, nearly eliminating peaks from solvent and exchangeable protons. A representative fit for isoleucine is shown in Figure 1. The resonances are defined as shown in Table 1 and parameters derived from the fit are shown in Tables 1-3. The HA, HG2, and HD1 resonances are each affected by only one or two ^3J couplings, making their relatively simple multiplet patterns easy to resolve. The HG12 and HG13 resonances add a mutual ^2J coupling and a ^3J coupling to the HB atom. The HG12/HG13 chemical shift difference of 104.7 Hz (relative to the -13.5 Hz ^2J coupling) is sufficient to minimize roofing effects from strong coupling in the experimental data (black), which shows minimal deviation from the modeled contribution of each resonance (gray and yellow, respectively). Despite a very complicated multiplet pattern for the HB atom (a doublet of doublets of doublets of quartets, blue), the resonance is very well fit by the model due to the couplings being shared with resonances having much less complexity.

Fits for all twenty amino acids are shown in Figure 2. Similar to isoleucine, the relatively simple spectra for glycine, alanine, valine, and threonine are all fit quite well and do not show significant strong coupling effects. The same is true of tryptophan, which has eight distinct resonances but only very slight strong coupling between HB2 and HB3.

https://doi.org/10.5194/mr-2024-7
Preprint. Discussion started: 9 April 2024

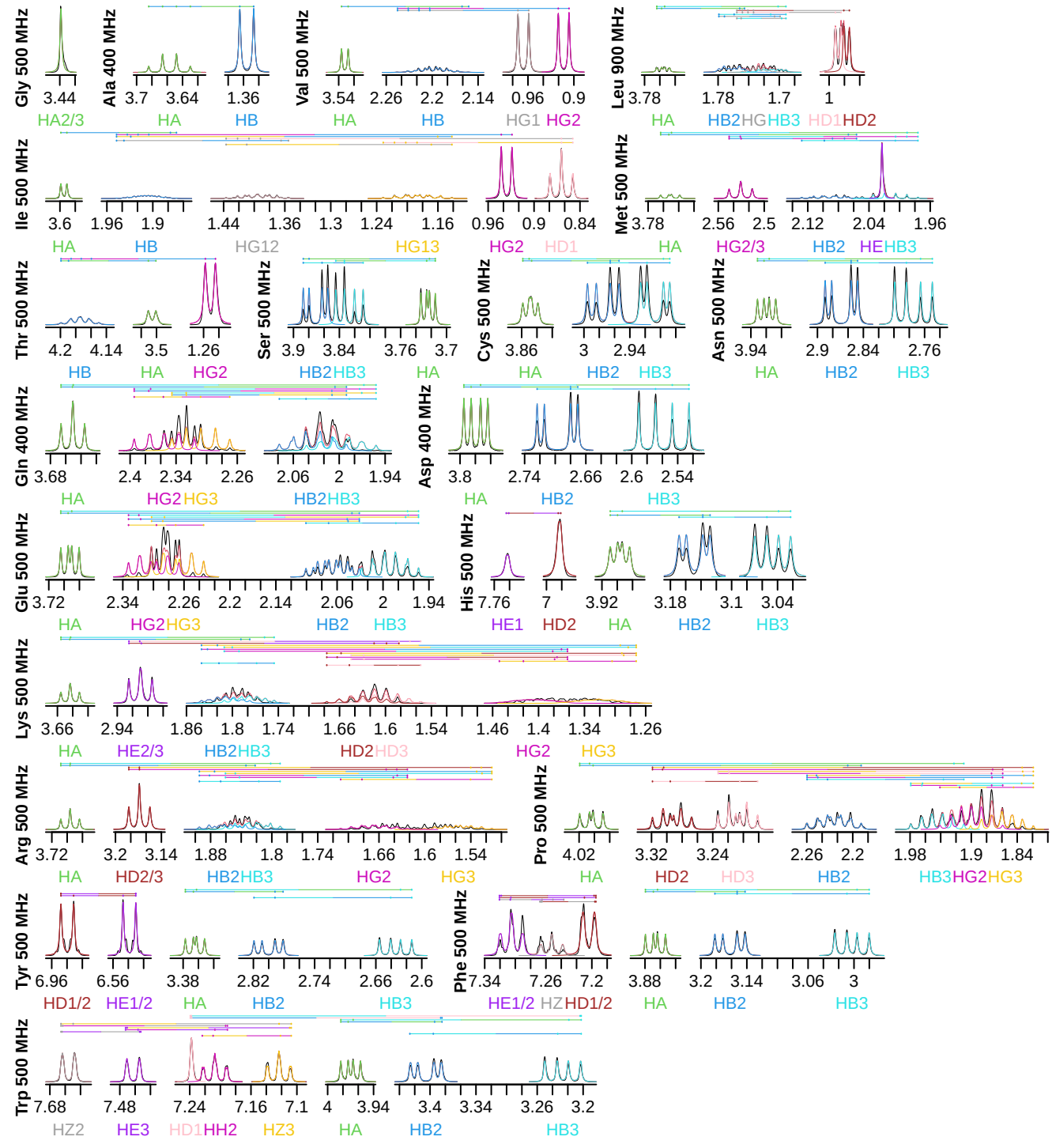

Figure 2. Fits of ^{1}H NMR spectra of all twenty canonical amino acids in D_2O. Spectra are plotted as described in Figure 1. The total modeled sum of all resonance contributions is shown in red, which is usually obscured by the individual contributions.

https://doi.org/10.5194/mr-2024-7
Preprint. Discussion started: 9 April 2024


Open Access MAGNETIC RESONANCE Discussions

Strong coupling is more pronounced in the beta protons of serine, cysteine, asparagine, and aspartate. These four side chains have the same three protons in the spectra, with HB2 and HB3 showing significant roofing effects. However, the multiplet patterns are easily resolved and the weak coupling model used by FitNMR finds an intermediate intensity between the two doublets. Despite not modeling the roofing effect, the linewidths do not appear to be distorted by the intensity mismatch. Histidine is largely similar with the addition of HD2 and HE1 nuclei in the imidazole ring that are only coupled to one another via a 1.7 Hz ^{4}J coupling.

Glutamine and glutamate add HG2 and HG3 nuclei, each with similar but distinct chemical shifts leading to large strong coupling effects. This results in outer multiplet peaks nearly disappearing. In proline, the HG2 and HG3 nuclei also have very similar chemical shifts and are quite strongly coupled. For methionine, the HG2 and HG3 nuclei appear to have indistinguishable chemical shifts and very similar scalar couplings, producing two overlapping, near-canonical triplets.

Leucine, with one HG atom, has two terminal methyl groups, each represented by a single resonance (HD1 or HD2). These make the multiplet pattern for HG quite complex. Due to the very similar ^{3}J(HG-HD1) and ^{3}J(HG-HD2) coupling constants (6.6 and 6.5 Hz, respectively), it is essentially a doublet of doublets of septets. Together with significant overlap between HB2, HB3, and HG (forming a strong coupling network between the three nuclei), this makes fitting the spectrum in this region very difficult. However, it is made somewhat easier because couplings involving the more isolated HA, HD1, and HD2 can be more easily resolved.

Tyrosine and phenylalanine also have somewhat complicated coupling networks in their aromatic rings, with four and five strongly coupled nuclei, respectively. They should each theoretically have both ^{3}J(HD1-HE1 or HD2-HE2) and ^{5}J(HD1-HE2 or HD2-HE1) couplings. In a purely weak coupling model, that would create a doublet of doublets for HD1/2 and HE1/2 in tyrosine. However, the experimental spectrum (black) shows what appears to be a doublet of triplets. The triplet behavior observed in the tyrosine spectrum arises due to the strong coupling network. During fitting, ^{5}J(HD-HE) drops to less than 0.0001 Hz, represented by the topmost vertical line. The phenylalanine fit does obtain reasonable values of 1.2 and 0.7 Hz for ^{5}J(HD-HE) and ^{4}J(HD-HZ), respectively. However, triplet behavior is still observed in the experimental spectrum, particularly for HE1/2, and remains unexplained by the weak coupling model.

Lysine, arginine, and proline are all capable of having distinct proton chemicals shifts at the beta, gamma, and delta positions. Distinct chemical shifts are observed for all such protons except for the HD2 and HD3 atoms in arginine. They show identical chemical shifts and produce a near perfect triplet, suggesting that the scalar couplings they make with HG2 and HG3 rotationally average out to near-identical values. The values of those scalar couplings and rotational averaging will be discussed in more detail below. While nearly all resonances in proline are modeled well, lysine and arginine are more difficult, especially for the HG2 and HG3 atoms, each of which are coupled to five nuclei.

Our data show that the large majority of protons in amino acid side chains can be modeled well using the FitNMR weak coupling approximation. However, peak overlap is an issue for several nuclei, suggesting 2D proton spectra like a NOESY or DQF-COSY may be required for adequate resolution. In addition, FitNMR and similar methods would benefit from incorporation of quantum mechanical calculations to enable accounting for strong coupling in the spectra.

https://doi.org/10.5194/mr-2024-7
Preprint. Discussion started: 9 April 2024

Open Access MAGNETIC RESONANCE Discussions

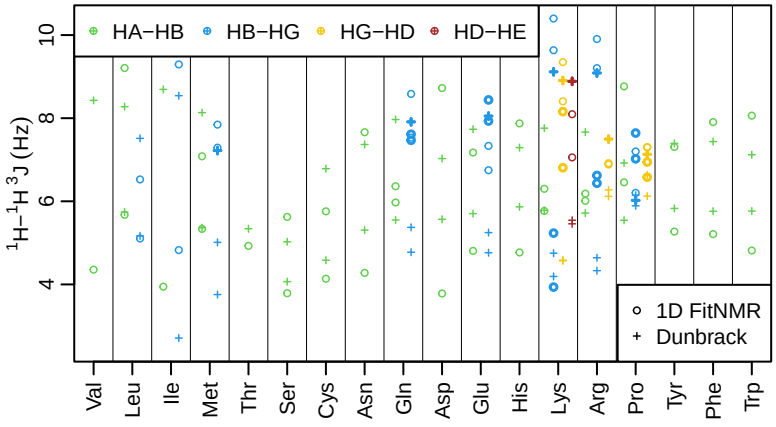

Figure 3. Side chain ^{1}H−^{1}H ^{3}J scalar couplings that depend on chi angles through the Karplus relationship. Couplings from fits of the 1D NMR spectra are shown with circles. Theoretical couplings calculated from the dataset used to create the 2010 Dunbrack rotamer library are shown with plus signs. HA-HB couplings are shown in green, HB-HG couplings are shown in blue, HG-HD couplings are shown in yellow, and HD-HE couplings are shown in auburn. The dihedral angles governing ^{3}J(HB2-HG2) and ^{3}J(HB3-HG3) have the same $\Delta\chi$ (see Table A2) and therefore should theoretically have the same value. The same is true for the corresponding HG-HD and HD-HE couplings. The symbols for these equivalent couplings are drawn with thick lines.

3.2 Chi angle-dependent side chain scalar couplings

Karplus parameters are required to derive structural information from scalar couplings. For ^3J couplings between adjacent CH_2 groups, the four proton-proton couplings completely sample all three values of $\Delta\chi$ (see chi 2-4 parameters in Table A2). In principle, this makes self-consistent Karplus parameterization possible given a sufficiently large number of ^3J(H-H) scalar coupling measurements across a diverse range of local geometries that have been stereospecifically assigned.

However, because of the small number of dihedral angles analyzed in this study and the lack of stereospecific assignments, we did not attempt such an analysis. Instead, we extrapolated parameters derived from scalar couplings associated with chi 1 (Pérez et al., 2001) to chi 2-4. We also did not attempt a reparameterization of C_0 and $\Delta C_{0,\mathrm{N}}$ (see Methods section 2.3) to account for the absence of a nitrogen substitution at chi 2 (in leucine, isoleucine, methionine, glutamine, glutamate, lysine, arginine, and proline) or chi 3 (in lysine).

The fit-derived ^3J couplings dependent on a side chain chi angle are shown as circles in Figure 3. There are eight amino acids with chi 2-related couplings (blue), three amino acids with chi 3-related couplings (yellow), and one with chi 4-related couplings (auburn). For chi angles with CH_2 groups on both sides of the associated rotatable bond, there are two couplings that in principle should take the same value due to having the same $\Delta\chi$ offset (see Table A2). These scalar couplings, shown with thicker symbols, were obtained without any constraint on their similarity in the software nor human knowledge of the expected equivalence during manual optimization of the input parameters. Despite that and the lack of stereospecific assignments, such

https://doi.org/10.5194/mr-2024-7
Preprint. Discussion started: 9 April 2024


Open Access MAGNETIC RESONANCE Discussions

equivalent couplings were within about 1 Hz of each other in all but one case (lysine HG-HD), supporting the relative accuracy of our approach despite the limitations.

As an initial point of comparison, we used the 2010 Dunbrak rotamer library dataset to calculate theoretical scalar couplings assuming the same chi angle distributions observed in crystal structures. These are shown as plus signs, with each thick plus sign representing the two scalar couplings with equivalent $\Delta\chi$ offsets. While the lack of stereospecific assignment in the experimental data makes a one-to-one comparison inappropriate for most couplings, the equivalent (thick) couplings can be unambiguously compared with the rotamer library couplings.

For these geometrically equivalent couplings, the experimental and rotamer library couplings are generally within about 1.5 Hz of each other. The exceptions are the lysine and arginine ^3J(HB-HG) values (blue), with the isolated amino acid data indicating a gauche chi 2 angle (low ^3J) while rotamer statistics favor a trans chi 2 angle (high ^3J). Beta-branched amino acids have just a single coupling associated with chi 1, allowing a similarly unambiguous comparison. Of these, the experimental and rotamer library couplings are very similar for threonine. However, the couplings for valine and isoleucine are quite different, suggesting some combination of the charged termini, absence of neighboring amino acid residues, or solvent exposure alters the free energy of these hydrophobic residues when isolated in solution.

Many of the experimentally measured scalar couplings with ambiguous assignments have rotamer library values somewhat nearby, providing less support for (but not necessarily excluding) differences in the energetic preferences. One possible systematic divergence between the experimental and rotamer-derived couplings was in the absolute difference between the two HA-HB couplings, Δ^3J(HA-HB) = $|^3$J(HA-HB2) $-$ ^{3}J(HA-HB3)|, which is especially pronounced for aspartate. However, with the experimental Δ^3J(HA-HB) value being greater than the rotamer library value for 10 out of 15 residues, the difference was not statistically significant (p = 0.20).

3.3 Analysis of chi 1 angle distributions

To more quantitatively model distributions of the chi 1 angle, for which the most reliable Karplus parameters were available, we used several different models of motion. The first, M_1, models chi angle fluctuations as being normally distributed with standard deviations ranging from 0-50°. During development of the previously published Karplus parameters used here, both the Karplus parameters and the M_1 model parameters ($\chi 1$ and $\sigma_{\chi 1}$) describing each experimentally measured residue were jointly optimized to be self-consistent with one another. (Pérez et al., 2001)

For the full range of $\chi 1$ and $\sigma_{\chi 1}$ values, we calculated the root mean squared error (RMSE) between the back-calculated and experimentally measured scalar couplings. Those are shown in Figure 4 as rectangular contour plots. For evaluation of the different models, we made no assumption about the stereospecific assignments of the HB2 and HB3 atoms. The RMSE values were calculated for both possible assignments and the minimum RMSE for a given set of model parameters is shown. Boundaries between regions with different assignments are drawn as dashed lines. For the beta-branched amino acids (valine, isoleucine, and threonine), there is no such ambiguity but the single scalar coupling provides less information.

The chi 1 distributions used by the Dunbrack rotamer library are shown in blue on top of each contour plot. For reference, we determined the M_1 model parameters that produced the closest distribution (in terms of the Bhattacharyya distance) to

https://doi.org/10.5194/mr-2024-7
Preprint. Discussion started: 9 April 2024

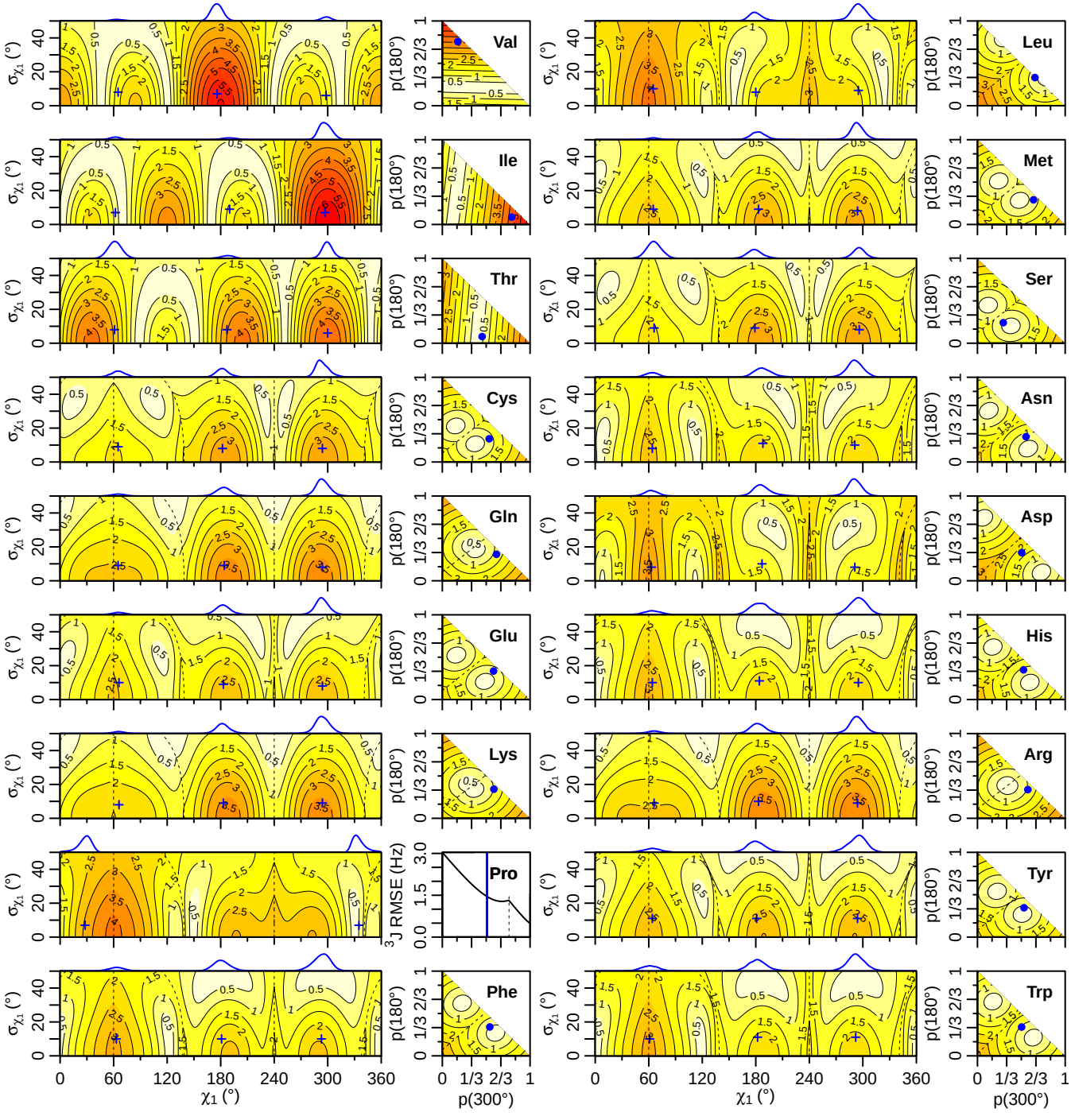

Figure 4. ^{3}J(HA-HB) root mean squared error (RMSE) in Hz for M_1 (left) and M_3 (right) models of motion. Dashed lines separate regions with swapped assignments. Dunbrack rotamer library distributions are shown on top of the M_1 plots, with the M_1 model having the closest match to each shown with a blue plus sign. Rotamer library populations are shown as a blue point or solid vertical line in the M_3 plots.

https://doi.org/10.5194/mr-2024-7
Preprint. Discussion started: 9 April 2024


Open Access MAGNETIC RESONANCE Discussions

each rotameric bin distribution. Those parameters are shown with blue plus signs. For amino acids excluding proline, the mean angles matching the rotamer library distributions (ranging 61-66°, 176-190°, 291-300°) were close to the canonical values. Due to the need for ring closure, the proline chi 1 angle distributions are skewed towards 0° or 360° and report primarily on ring pucker. The standard deviations of the rotamer library distributions ranged 6-11°, with ringed side chains having the most variation ($\sigma_{\chi 1} \geq 10°$).

While $\sigma_{\chi 1}$ was varied 0-50° both here and in the original Karplus parameterization, $\sigma_{\chi 1}$ values much greater than those observed in the PDB are not physically realistic. Furthermore, mean angles too far from those observed in the PDB are also not likely. The applicability of the unimodal M_1 model to the experimental data can be judged based on how nearby a region with low RMSE is to the blue plus sign. For nearly all of the amino acids, the measured ^3J(HA-HB) couplings are sufficient to exclude the M_1 model, suggesting that they instead populate multiple rotamer bins as would be expected for an isolated amino acid in solution. Proline does show a set of M_1 parameters very close to a rotamer library distribution. Isoleucine is the only other amino acid where the single-rotamer model could be considered reasonable (with a plus symbol RMSE < 1 Hz), likely due to the reduced information content of the single scalar coupling.

An alternate M_2 model was previously tested that back-calculated the scalar couplings using a population-weighted mean of the theoretical scalar couplings at 60°, 180°, and 300°, which also makes it a two-parameter model. (Pérez et al., 2001) However, as the Dunbrack rotamer library indicates, side chains generally sample a range of values within a rotamer well. In addition, there is an amino acid-specific bias away from the canonical angles, which can be subtle for many amino acids but quite large for proline. To account for this prior information, we propose another two-parameter model, referred to here as M_3, that uses average scalar couplings calculated directly from the rotameric bins in the Dunbrack 2010 rotamer library dataset.

The RMSE values for the M_3 model are shown as square contour plots in Figure 4, with the populations from the rotamer library shown as a blue point. Because only two valid rotamers exist for proline, the RMSE is plotted as a line vs. the population of the 300° (gauche minus) rotamer, with the rotamer library population shown as a vertical blue line.

For the M_1 model, which allows chi angles with unrealistically high potential energies, it is possible to judge model applicability by comparing with rotamer library distributions (i.e. blue plus signs). However, because the M_3 model stays within observable chi angles by definition, there is not necessarily a means to assess model validity with *a priori* information. However, the vast majority of isolated amino acids do have scalar couplings reasonably consistent (RMSE < 1 Hz) with the rotamer library populations, which is not necessarily expected given the presence of the NH_3^+ and COO^- groups, lack of neighboring amino acids, and high solvent exposure.

By contrast, beta-branched valine and isoleucine have ^3J(HA-HB) values quite inconsistent with the rotamer populations observed in the PDB. The $\chi 1 = 180°$ rotamer of valine and $\chi 1 = 300°$ rotamer of isoleucine, both highly populated in the PDB, have very similar three-dimensional structures due to differences in the way chi 1 atoms are defined. (Figure 5A/B) These rotamers are likely very prevalent in folded proteins because they avoid more strained conformations where either gamma carbon has two gauche interactions with the backbone. Interestingly, the threonine $\chi 1 = 300°$ rotamer that has a similar heavy atom arrangement (Figure 4C) appears to have a population slightly under 50% in solution according to the M_3 model. (Figure

https://doi.org/10.5194/mr-2024-7
Preprint. Discussion started: 9 April 2024

Open Access MAGNETIC RESONANCE Discussions

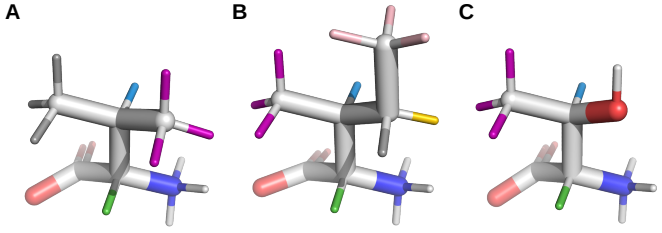

Figure 5. Beta-branched amino acids, with hydrogen colors matching those used in Figures 1 and 2. ^{3}J(HA-HB) is most sensitive to the population of the shown rotamers because HA (green) is trans to HB (blue), giving the maximum theoretical scalar coupling. **A)** Valine $\chi1 = 180°$ rotamer. **B)** Isoleucine $\chi1 = 300°$ rotamer. **C)** Threonine $\chi1 = 300°$ rotamer. The hydroxyl hydrogen (white) was also deuterated in the sample.

4) The differences in preferences for these rotamers in the isolated amino acids could arise due to the more hydrophobic side chains of valine and isoleucine imposing a greater desolvation penalty on the NH_3^+ group than threonine does.

Proline is another amino acid whose PDB populations are not consistent with those observed for the isolated amino acid. Whereas crystal structures show nearly equal populations of the C_γ exo ($\chi1 \approx 30°$) and C_γ endo ($\chi1 \approx 330°$), solution NMR of the isolated amio acid shows a strong preference for the C_γ exo conformation. Aspartate also shows a stronger preference for either the $\chi1 = 180°$ or $\chi1 = 300°$ rotamers when isolated in solution than it does in folded crystal structures.

Finally, several amino acids show near uniform populations of their three different chi 1 rotamers in solution, including lysine, arginine, and glutamine. All three side chains have longer aliphatic substructures, $(CH_2)_{2-4}$, and positively charged or polar head groups, which may contribute to the relatively equal rotameric free energies.

4 Conclusions

Our results indicate that for most nuclei, the weak-coupling assumption yields useful information about side chain dihedral angles. Only a small subset of nuclei show strong coupling and for nearly all that do, it is a geminal ^{2}J coupling that does not contain readily quantifiable structural information. For the aliphatic regions of longer side chains where such ^{2}J couplings are also involved in ^{3}J couplings, strong coupling has a larger impact on structural analysis. To fully capture the complexity of multiplet patterns observed for such amino acid side chains, a strong coupling model is required. Even in multidimensional spectra that have insufficient resolution to accurately quantify scalar couplings through computational analysis, having an accurate model of the asymmetry is likely important for quantifying the volumes of severely overlapped peaks, for instance in a 2D or 3D NOESY. As such, incorporation of a quantum mechanical spin system model into FitNMR is in progress.

The generalized strategy of parameterizing Karplus coefficients using the number of heavy-atom substitutions (Pérez et al., 2001) appears to produce reasonable agreement between experiment and theory when extrapolated to chi 2-4, which were not part of the original training data. This strategy is likely applicable to non-protein small molecules as well. Given a sufficiently

https://doi.org/10.5194/mr-2024-7
Preprint. Discussion started: 9 April 2024


Open Access MAGNETIC RESONANCE Discussions

large dataset of proton-proton couplings with stereospecific assignments, the parameterization could be further tested and perhaps improved through additional self-consistent optimization.

By mapping out the full parameter space of motion models assuming the absence (M_1) or presence (M_3) of multiple rotamers, much can be learned about side chain motion or lack thereof. As we illustrate here, differentiating between the models requires a minimum of two scalar couplings per bond. While helpful for maximum information content, stereospecific assignments do not appear strictly necessary to demonstrate the presence of multiple rotamers. While there are multiple purely heavy atom scalar couplings associated with the chi 1 angle, the same is not true for most chi 2-4 angles. This illustrates the power of proton spectral analysis and provides motivation for further development in this area.

As shown here, peak overlap is already an issue for interpreting coupling constants from 1D spectra of individual amino acids. Overlap becomes prohibitive in 1D spectra of folded proteins but can likely be overcome to a large extent through the use of multidimensional $^1H-^1H$ 2D spectra like the NOESY, which contain at least one isolated cross-peak for many nuclei. Without the presence of isotopically labeled heteronuclei requiring decoupling, the receiver can be left open during direct-dimension acquisition, allowing access to the complete free induction decay (FID). For small, single-digit kDa proteins, the multiplet patterns may be accessible to software like FitNMR in a similar manner to the ^3J(H-HA) doublet. (Dudley et al., 2020) A relatively new class of proteins that size are computationally designed miniprotein binders, which are able to target therapeutically relevant proteins (Cao et al., 2022) and also are quite accessible to NMR characterization (Dudley et al., 2024). Larger proteins may benefit from a strategy analogous to previously employed techniques (Oschkinat and Freeman, 1984; Kessler et al., 1985; Titman and Keeler, 1990; Huber et al., 1993; Prasch et al., 1998) of analyzing in-phase data together with anti-phase data from experiments like the DQF-COSY, where the observed signal intensity is proportional to the degree of anti-phase splitting by the coupling active in the cross-peak (Delaglio et al., 2001). Such spectra have historically been applied to the assignment and analysis of smaller unlabeled polypeptides (Wüthrich, 1986; Inagaki, 2013) but not fully exploited for their structural information content. This study lays the groundwork for comprehensive modeling and structural interpretation of multiplets in multidimensional protein spectra.

Code and data availability. This manuscript was prepared using R Markdown. All code and data required for reproducing the manuscript, figures, and tables in their entirety are available in the supplement ZIP archive distributed with the paper. See the README.md file within for more details. The fitting methodology is implemented in the FitNMR open-source R package. https://github.com/smith-group/fitnmr

https://doi.org/10.5194/mr-2024-7
Preprint. Discussion started: 9 April 2024


Open Access MAGNETIC RESONANCE Discussions

Appendix A: Supplementary information

A1 Processing amino acid 1D NMR data

Amino acid 1D NMR free induction decay (FID) data were converted and processed using NMRPipe. FID conversion was performed using the `bruker` program, with chemical shift referencing done using the temperature dependence of the H_2O chemical shift. Temperatures ranged 298-306 K depending on the amino acid sample (see Table A1). Spectra were processed with the following NMRPipe script, which includes a cosine window function and frequency domain polynomial baseline correction:

```
#!/bin/csh

nmrPipe -in test.fid \
| nmrPipe  -fn SP -off 0.5 -end 1.00 -pow 1 -c 0.5    \
| nmrPipe  -fn ZF -auto                               \
| nmrPipe  -fn FT -auto                               \
| nmrPipe  -fn PS -p0 $P0 -p1 $P1 -di -verb           \
| nmrPipe  -fn POLY -auto                             \
   -ov -out test.ft1
```

The zero- and first-order phases were extracted from the original TopSpin processing parameters. Their signs were changed prior to insertion into the NMRPipe script above. The Bruker PHC0 and PHC1 parameters were extracted using the following commands:

```
grep PHC0 pdata/1/proc | cut -d " " -f 2
grep PHC1 pdata/1/proc | cut -d " " -f 2
```

https://doi.org/10.5194/mr-2024-7
Preprint. Discussion started: 9 April 2024

Open Access MAGNETIC RESONANCE Discussions

Table A1. Amino acid data used from the BMRB. Temperatures shown are from recorded Bruker acquisition parameters.

Amino Acid	Field Strength (MHz)	Temperature (K)	BMRB ID
Ala	400	306	bmse000028
Arg	500	298	bmse000029
Asn	500	298	bmse000030
Asp	400	306	bmse000031
Cys	500	298	bmse000034
Gln	400	306	bmse000038
Glu	500	298.16	bmse000037
Gly	500	298	bmse000089
His	500	298	bmse000039
Ile	500	298	bmse000041
Leu	900	298	bmse000042
Lys	500	298	bmse000043
Met	500	298	bmse000044
Phe	500	298	bmse000045
Pro	500	298	bmse000047
Ser	500	298	bmse000048
Thr	500	298	bmse000049
Trp	500	298	bmse000050
Tyr	500	298.16	bmse000051
Val	500	298	bmse000052

https://doi.org/10.5194/mr-2024-7
Preprint. Discussion started: 9 April 2024

Open Access MAGNETIC RESONANCE Discussions

Table A2. Data for creating Karplus parameters for ^{1}H-^{1}H ^{3}J couplings. N_i give number of each heavy atom bonded to central atom pair.

AA	χ #	$\Delta\chi$	H_1	H_2	N_C	N_N	N_O	N_S	AA	χ #	$\Delta\chi$	H_1	H_2	N_C	N_N	N_O	N_S
Val	1	0	HA	HB	3	1	0	0	Lys	2	0	HB2	HG2	2	0	0	0
Leu	1	-120	HA	HB2	2	1	0	0	Lys	2	120	HB2	HG3	2	0	0	0
Leu	1	0	HA	HB3	2	1	0	0	Lys	2	-120	HB3	HG2	2	0	0	0
Leu	2	120	HB2	HG	3	0	0	0	Lys	2	0	HB3	HG3	2	0	0	0
Leu	2	0	HB3	HG	3	0	0	0	Lys	3	0	HG2	HD2	2	0	0	0
Ile	1	-120	HA	HB	3	1	0	0	Lys	3	120	HG2	HD3	2	0	0	0
Ile	2	0	HB	HG12	3	0	0	0	Lys	3	-120	HG3	HD2	2	0	0	0
Ile	2	120	HB	HG13	3	0	0	0	Lys	3	0	HG3	HD3	2	0	0	0
Met	1	-120	HA	HB2	2	1	0	0	Lys	4	0	HD2	HE2	1	1	0	0
Met	1	0	HA	HB3	2	1	0	0	Lys	4	120	HD2	HE3	1	1	0	0
Met	2	0	HB2	HG2	1	0	0	1	Lys	4	-120	HD3	HE2	1	1	0	0
Met	2	120	HB2	HG3	1	0	0	1	Lys	4	0	HD3	HE3	1	1	0	0
Met	2	-120	HB3	HG2	1	0	0	1	Arg	1	-120	HA	HB2	2	1	0	0
Met	2	0	HB3	HG3	1	0	0	1	Arg	1	0	HA	HB3	2	1	0	0
Thr	1	-120	HA	HB	2	1	1	0	Arg	2	0	HB2	HG2	2	0	0	0
Ser	1	-120	HA	HB2	1	1	1	0	Arg	2	120	HB2	HG3	2	0	0	0
Ser	1	0	HA	HB3	1	1	1	0	Arg	2	-120	HB3	HG2	2	0	0	0
Cys	1	-120	HA	HB2	1	1	0	1	Arg	2	0	HB3	HG3	2	0	0	0
Cys	1	0	HA	HB3	1	1	0	1	Arg	3	0	HG2	HD2	1	1	0	0
Asn	1	-120	HA	HB2	2	1	0	0	Arg	3	120	HG2	HD3	1	1	0	0
Asn	1	0	HA	HB3	2	1	0	0	Arg	3	-120	HG3	HD2	1	1	0	0
Gln	1	-120	HA	HB2	2	1	0	0	Arg	3	0	HG3	HD3	1	1	0	0
Gln	1	0	HA	HB3	2	1	0	0	Pro	1	-120	HA	HB2	2	1	0	0
Gln	2	0	HB2	HG2	2	0	0	0	Pro	1	0	HA	HB3	2	1	0	0
Gln	2	120	HB2	HG3	2	0	0	0	Pro	2	0	HB2	HG2	2	0	0	0
Gln	2	-120	HB3	HG2	2	0	0	0	Pro	2	120	HB2	HG3	2	0	0	0
Gln	2	0	HB3	HG3	2	0	0	0	Pro	2	-120	HB3	HG2	2	0	0	0
Asp	1	-120	HA	HB2	2	1	0	0	Pro	2	0	HB3	HG3	2	0	0	0
Asp	1	0	HA	HB3	2	1	0	0	Pro	3	0	HG2	HD2	1	1	0	0
Glu	1	-120	HA	HB2	2	1	0	0	Pro	3	120	HG2	HD3	1	1	0	0
Glu	1	0	HA	HB3	2	1	0	0	Pro	3	-120	HG3	HD2	1	1	0	0
Glu	2	0	HB2	HG2	2	0	0	0	Pro	3	0	HG3	HD3	1	1	0	0
Glu	2	120	HB2	HG3	2	0	0	0	Tyr	1	-120	HA	HB2	2	1	0	0
Glu	2	-120	HB3	HG2	2	0	0	0	Tyr	1	0	HA	HB3	2	1	0	0
Glu	2	0	HB3	HG3	2	0	0	0	Phe	1	-120	HA	HB2	2	1	0	0
His	1	-120	HA	HB2	2	1	0	0	Phe	1	0	HA	HB3	2	1	0	0
His	1	0	HA	HB3	2	1	0	0	Trp	1	-120	HA	HB2	2	1	0	0
Lys	1	-120	HA	HB2	2	1	0	0	Trp	1	0	HA	HB3	2	1	0	0
Lys	1	0	HA	HB3	2	1	0	0									

https://doi.org/10.5194/mr-2024-7
Preprint. Discussion started: 9 April 2024

Open Access MAGNETIC RESONANCE Discussions

Author contributions. NRS and NBM did fits of the 1D NMR spectra. CAS did the other analyses and wrote the manuscript.

Competing interests. The authors declare no competing interests.

Disclaimer. Publisher's note: Copernicus Publications remains neutral with regard to jurisdictional claims in published maps and institutional affiliations.

Acknowledgements. This work was supported by NIH grant 1R15GM141974-01.

https://doi.org/10.5194/mr-2024-7
Preprint. Discussion started: 9 April 2024

Open Access MAGNETIC RESONANCE Discussions

References

Achanta, P. S., Jaki, B. U., McAlpine, J. B., Friesen, J. B., Niemitz, M., Chen, S.-N., and Pauli, G. F.: Quantum mechanical NMR full spin analysis in pharmaceutical identity testing and quality control, Journal of Pharmaceutical and Biomedical Analysis, 192, 113 601, https://doi.org/10.1016/j.jpba.2020.113601, 2021.

Ahlner, A., Carlsson, M., Jonsson, B.-H., and Lundström, P.: PINT: a software for integration of peak volumes and extraction of relaxation rates, Journal of Biomolecular NMR, 56, 191–202, https://doi.org/10.1007/s10858-013-9737-7, 2013.

Bernstein, M. A., Sýkora, S., Peng, C., Barba, A., and Cobas, C.: Optimization and Automation of Quantitative NMR Data Extraction, Analytical Chemistry, 85, 5778–5786, https://doi.org/10.1021/ac400411q, 2013.

Cao, L., Coventry, B., Goreshnik, I., Huang, B., Sheffler, W., Park, J. S., Jude, K. M., Marković, I., Kadam, R. U., Verschueren, K. H. G., Verstraete, K., Walsh, S. T. R., Bennett, N., Phal, A., Yang, A., Kozodoy, L., DeWitt, M., Picton, L., Miller, L., Strauch, E.-M., DeBouver, N. D., Pires, A., Bera, A. K., Halabiya, S., Hammerson, B., Yang, W., Bernard, S., Stewart, L., Wilson, I. A., Ruohola-Baker, H., Schlessinger, J., Lee, S., Savvides, S. N., Garcia, K. C., and Baker, D.: Design of protein-binding proteins from the target structure alone, Nature, 605, 551–560, https://doi.org/10.1038/s41586-022-04654-9, 2022.

Castellano, S. and Bothner-By, A. A.: Analysis of NMR Spectra by Least Squares, The Journal of Chemical Physics, 41, 3863–3869, https://doi.org/10.1063/1.1725826, 1964.

Castillo, A. M., Patiny, L., and Wist, J.: Fast and accurate algorithm for the simulation of NMR spectra of large spin systems, Journal of Magnetic Resonance, 209, 123–130, https://doi.org/10.1016/j.jmr.2010.12.008, 2011.

Cheshkov, D. A. and Sinitsyn, D. O.: Chapter Two - Total line shape analysis of high-resolution NMR spectra, vol. 100, pp. 61–96, Academic Press, ISBN 0066-4103, https://doi.org/10.1016/bs.arnmr.2019.11.001, 2020.

Cheshkov, D. A., Sheberstov, K. F., Sinitsyn, D. O., and Chertkov, V. A.: ANATOLIA: NMR software for spectral analysis of total lineshape, Magnetic Resonance in Chemistry, 56, 449–457, https://doi.org/10.1002/mrc.4689, 2018.

Dashti, H., Westler, W. M., Tonelli, M., Wedell, J. R., Markley, J. L., and Eghbalnia, H. R.: Spin System Modeling of Nuclear Magnetic Resonance Spectra for Applications in Metabolomics and Small Molecule Screening., Anal Chem, 89, 12 201–12 208, https://doi.org/10.1021/acs.analchem.7b02884, 2017.

Dashti, H., Wedell, J. R., Westler, W. M., Tonelli, M., Aceti, D., Amarasinghe, G. K., Markley, J. L., and Eghbalnia, H. R.: Applications of Parametrized NMR Spin Systems of Small Molecules., Anal Chem, 90, 10 646–10 649, https://doi.org/10.1021/acs.analchem.8b02660, 2018.

Delaglio, F., Grzesiek, S., Vuister, G. W., Zhu, G., Pfeifer, J., and Bax, A.: NMRPipe: A multidimensional spectral processing system based on UNIX pipes, Journal of Biomolecular NMR, 6, 277–293, https://doi.org/10.1007/BF00197809, 1995.

Delaglio, F., Wu, Z., and Bax, A.: Measurement of Homonuclear Proton Couplings from Regular 2D COSY Spectra, Journal of Magnetic Resonance, 149, 276–281, https://doi.org/10.1006/jmre.2001.2297, 2001.

Dudley, J. A., Park, S., MacDonald, M. E., Fetene, E., and Smith, C. A.: Resolving overlapped signals with automated FitNMR analytical peak modeling, J Magn Reson, 318, 106 773, https://doi.org/10.1016/j.jmr.2020.106773, 2020.

Dudley, J. A., Park, S., Cho, O., Wells, N. G. M., MacDonald, M. E., Blejec, K. M., Fetene, E., Zanderigo, E., Houliston, S., Liddle, J. C., Dashnaw, C. M., Sabo, T. M., Shaw, B. F., Balsbaugh, J. L., Rocklin, G. J., and Smith, C. A.: Heat-induced structural and chemical changes to a computationally designed miniprotein, Protein Sci, 2024.

https://doi.org/10.5194/mr-2024-7
Preprint. Discussion started: 9 April 2024

Open Access MAGNETIC RESONANCE Discussions

Emerson, S. D. and Montelione, G. T.: 2D and 3D HCCH TOCSY experiments for determining 3J(HαHβ) coupling constants of amino acid residues, Journal of Magnetic Resonance (1969), 99, 413–420, https://doi.org/10.1016/0022-2364(92)90196-E, 1992.

Gemmecker, G. and Fesik, S. W.: A method for measuring 1H-1H coupling constants in 13C-labeled molecules, Journal of Magnetic Resonance (1969), 95, 208–213, https://doi.org/10.1016/0022-2364(91)90340-Y, 1991.

Griesinger, C. and Eggenberger, U.: Determination of proton-proton coupling constants in 13C-labeled molecules, Journal of Magnetic Resonance (1969), 97, 426–434, https://doi.org/10.1016/0022-2364(92)90328-5, 1992.

Griesinger, C., Sørensen, O. W., and Ernst, R. R.: Two-dimensional correlation of connected NMR transitions, Journal of the American Chemical Society, 107, 6394–6396, https://doi.org/10.1021/ja00308a042, 1985.

Griesinger, C., Sørensen, O. W., and Ernst, R. R.: Correlation of connected transitions by two-dimensional NMR spectroscopy, The Journal of Chemical Physics, 85, 6837–6852, https://doi.org/10.1063/1.451421, 1986.

Griesinger, C., Sørensen, O. W., and Ernst, R. R.: Practical aspects of the E.COSY technique. Measurement of scalar spin-spin coupling constants in peptides, Journal of Magnetic Resonance (1969), 75, 474–492, https://doi.org/10.1016/0022-2364(87)90102-8, 1987.

Grzesiek, S., Kuboniwa, H., Hinck, A. P., and Bax, A.: Multiple-Quantum Line Narrowing for Measurement of H.alpha.-H.beta. J Couplings in Isotopically Enriched Proteins, Journal of the American Chemical Society, 117, 5312–5315, https://doi.org/10.1021/ja00124a014, 1995.

Heinzer, J.: Iterative least-squares nmr lineshape fitting with use of symmetry and magnetic equivalence factorization, Journal of Magnetic Resonance (1969), 26, 301–316, https://doi.org/10.1016/0022-2364(77)90176-7, 1977.

Hoch, J. C., Baskaran, K., Burr, H., Chin, J., Eghbalnia, H. R., Fujiwara, T., Gryk, M. R., Iwata, T., Kojima, C., Kurisu, G., Maziuk, D., Miyanoiri, Y., Wedell, J. R., Wilburn, C., Yao, H., and Yokochi, M.: Biological Magnetic Resonance Data Bank, Nucleic Acids Res, 51, D368–D376, https://doi.org/10.1093/nar/gkac1050, 2023.

Hogben, H. J., Krzystyniak, M., Charnock, G. T. P., Hore, P. J., and Kuprov, I.: Spinach –A software library for simulation of spin dynamics in large spin systems, Journal of Magnetic Resonance, 208, 179–194, https://doi.org/10.1016/j.jmr.2010.11.008, 2011.

Huber, P., Zwahlen, C., Vincent, S. J. F., and Bodenhausen, G.: Accurate Determination of Scalar Couplings by Convolution of Complementary Two-Dimensional Multiplets, Journal of Magnetic Resonance, Series A, 103, 118–121, https://doi.org/10.1006/jmra.1993.1142, 1993.

Inagaki, F.: Protein NMR Resonance Assignment, pp. 2033–2037, Springer Berlin Heidelberg, Berlin, Heidelberg, ISBN 978-3-642-16712-6, https://doi.org/10.1007/978-3-642-16712-6_312, 2013.

Karplus, M.: Vicinal Proton Coupling in Nuclear Magnetic Resonance, Journal of the American Chemical Society, 85, 2870–2871, https://doi.org/10.1021/ja00901a059, 1963.

Kessler, H., Müller, A., and Oschkinat, H.: Differences and sums of traces within, COSY spectra (DISCO) for the extraction of coupling constants: 'Decoupling'after the measurement, Magnetic Resonance in Chemistry, 23, 844–852, https://doi.org/10.1002/mrc.1260231012, 1985.

Li, D.-W., Bruschweiler-Li, L., Hansen, A. L., and Brüschweiler, R.: DEEP Picker1D and Voigt Fitter1D: a versatile tool set for the automated quantitative spectral deconvolution of complex 1D-NMR spectra, Magnetic Resonance, 4, 19–26, https://doi.org/10.5194/mr-4-19-2023, 2023.

Löhr, F., Schmidt, J. M., and Rüterjans, H.: Simultaneous Measurement of 3JHN,H$\alpha$and 3JHα,HβCoupling Constants in 13C,15N-Labeled Proteins, Journal of the American Chemical Society, 121, 11 821–11 826, https://doi.org/10.1021/ja991356h, 1999.

Niklasson, M., Otten, R., Ahlner, A., Andresen, C., Schlagnitweit, J., Petzold, K., and Lundström, P.: Comprehensive analysis of NMR data using advanced line shape fitting, Journal of Biomolecular NMR, 69, 93–99, https://doi.org/10.1007/s10858-017-0141-6, 2017.

https://doi.org/10.5194/mr-2024-7
Preprint. Discussion started: 9 April 2024

Open Access MAGNETIC RESONANCE Discussions

Oschkinat, H. and Freeman, R.: Fine structure in two-dimensional NMR correlation spectroscopy, Journal of Magnetic Resonance (1969), 60, 164–169, https://doi.org/10.1016/0022-2364(84)90044-1, 1984.

Pérez, C., Löhr, F., Rüterjans, H., and Schmidt, J. M.: Self-consistent Karplus parametrization of 3J couplings depending on the polypeptide side-chain torsion chi1., J Am Chem Soc, 123, 7081–7093, https://doi.org/10.1021/ja003724j, 2001.

Prasch, T., Gröschke, P., and Glaser, S. J.: SIAM, a Novel NMR Experiment for the Determination of Homonuclear Coupling Constants, Angewandte Chemie International Edition, 37, 802–806, https://doi.org/10.1002/(SICI)1521-3773(19980403)37:6<802::AID-ANIE802>3.0.CO;2-M, 1998.

Schmidt, J. M., Blümel, M., Löhr, F., and Rüterjans, H.: Self-consistent 3J coupling analysis for the joint calibration of Karplus coefficients and evaluation of torsion angles, Journal of Biomolecular NMR, 14, 1–12, https://doi.org/10.1023/A:1008345303942, 1999.

Shapovalov, M. V. and Dunbrack, R. L.: A Smoothed Backbone-Dependent Rotamer Library for Proteins Derived from Adaptive Kernel Density Estimates and Regressions, Structure, 19, 844–858, https://doi.org/10.1016/j.str.2011.03.019, 2011.

Smith, A. A.: INFOS: spectrum fitting software for NMR analysis, Journal of Biomolecular NMR, 67, 77–94, https://doi.org/10.1007/s10858-016-0085-2, 2017.

Tessari, M., Mariani, M., Boelens, R., and Kaptein, R.: (H)XYH-COSY and (H)XYH-E.COSY Experiments for Backbone and Side-Chain Assignment and Determination of 3JHH′Coupling Constants in (13C, 15N)-Labeled Proteins, Journal of Magnetic Resonance, Series B, 108, 89–93, https://doi.org/10.1006/jmrb.1995.1108, 1995.

Tiainen, M., Soininen, P., and Laatikainen, R.: Quantitative Quantum Mechanical Spectral Analysis (qQMSA) of 1H NMR spectra of complex mixtures and biofluids, Journal of Magnetic Resonance, 242, 67–78, https://doi.org/10.1016/j.jmr.2014.02.008, 2014.

Titman, J. J. and Keeler, J.: Measurement of homonuclear coupling constants from NMR correlation spectra, Journal of Magnetic Resonance (1969), 89, 640–646, https://doi.org/10.1016/0022-2364(90)90351-9, 1990.

Veshtort, M. and Griffin, R. G.: SPINEVOLUTION: A powerful tool for the simulation of solid and liquid state NMR experiments, Journal of Magnetic Resonance, 178, 248–282, https://doi.org/10.1016/j.jmr.2005.07.018, 2006.

Vuister, G. W. and Bax, A.: Quantitative J correlation: a new approach for measuring homonuclear three-bond J(HNH.alpha.) coupling constants in 15N-enriched proteins, Journal of the American Chemical Society, 115, 7772–7777, https://doi.org/10.1021/ja00070a024, 1993.

Vuister, G. W., Tessari, M., Karimi-Nejad, Y., and Whitehead, B.: Pulse Sequences for Measuring Coupling Constants, pp. 195–257, Springer US, Boston, MA, ISBN 978-0-306-47083-7, https://doi.org/10.1007/0-306-47083-7_6, 2002.

Westbrook, J. D., Shao, C., Feng, Z., Zhuravleva, M., Velankar, S., and Young, J.: The chemical component dictionary: complete descriptions of constituent molecules in experimentally determined 3D macromolecules in the Protein Data Bank, Bioinformatics, 31, 1274–1278, https://doi.org/10.1093/bioinformatics/btu789, 2015.

Wüthrich, K.: NMR of proteins and nucleic acids, Wiley, New York, ISBN 0471828939, 1986.